Influence of nalidixic acid on tandem heterotrophic-autotrophic kinetics in a

"NIPHO" activated sludge reactor

J.C. Leyva-Díaz [a], R.A. Phonbun [b], J. Taggart [b], E. Díaz [a], S. Ordóñez [a*]

[a] Department of Chemical and Environmental Engineering, University of Oviedo, 33006 Oviedo, Spain

[b] Department of Chemical and Process Engineering, University of Strathclyde, G11XJ Glasgow, United Kingdom

[*] corresponding author, email: sordonez@uniovi.es, phone number: +34 985103437, Department of Chemical and Environmental Engineering, University of Oviedo, 33006 Oviedo, Spain

ABSTRACT

This work analyzes the effect of nalidixic acid (NAL) on the kinetics of the heterotrophic and autotrophic biomass growth within a "NIPHO" activated sludge reactor treating municipal wastewater. Thus, the effect of this chemical in the degradation rates of carbon and nitrogen sources and net biomass growth rate is evaluated. Activated sludge samples were taken at three different operation conditions, changing the values of hydraulic retention time (2.8-3.8 h), biomass concentration (1,400-1,700 mgVSS L^{-1}), temperature (12.6-14.8ºC), and sludge retention time (11.0-12.6 day). A respirometric method was applied to model the kinetic performance of heterotrophic and autotrophic biomass in absence and presence of NAL, and a multivariable statistical analysis was carried out to characterize the influence of the operation variables on the kinetic response of the system, which was finally optimized. The results showed that there was no inhibitory effect of NAL on heterotrophic biomass, with an increase of net heterotrophic biomass growth rate from 1.70 to 6.73 mgVSS L^{-1} h^{-1} at the most favorable period. By contrast, the autotrophic biomass was negatively affected by NAL, reducing the value of net autotrophic biomass growth rate from 25.37 to 10.29 mgVSS L^{-1} h^{-1} at the best operation conditions. In general, biomass concentration and temperature had the highest influence on the degradation rate of

27 carbon and nitrogen sources, whereas hydraulic retention time and sludge retention time

28 were the most influential on net heterotrophic and autotrophic biomass growth rates.

29 **Keywords:** Activated sludge reactor; Autotrophic biomass; Heterotrophic biomass;

30 Kinetic modeling; Nalidixic acid; Respirometry.

31

32 1. INTRODUCTION

33 In the last years, pharmaceuticals have caused a growing concern due to their presence

34 and environmental persistence. Among these compounds, it should be highlighted the

35 antibiotics, which are used in human medicine, animal husbandry and agriculture

36 (Tahrani et al., 2015; Lekunberri et al., 2017). Since last decade, global consumption

37 and use of antibiotics raised from 50 to 70 billion standard units approximately

38 (Gelbrand et al., 2015). As a consequence of their extensive application, antibiotic

39 residues are continuously introduced into the environment through different ways, such

40 as the effluents from wastewater treatment plants (WWTPs), surface runoff and soil

41 leaching (Park and Choi, 2008; Servais and Passerat, 2009; Zhang et al., 2009, Mojica

42 and Aga, 2011). In light of this, antibiotic contamination is recognized as an emerging

43 environmental pollution in aquatic environments due to their potential adverse effects

44 on the ecosystem and human health (Huang et al., 2001; Kummerer, 2009; Yang et al.,

45 2011). In particular, despite the fact that antibiotics have toxic effects, the main problem

46 related to the presence of lot of these compounds in the environment is the development

47 of antibiotic-resistant microorganisms, which is the real problem affecting human

48 health.

49 Among the most widely used antibiotics worldwide, nalidixic acid (NAL), a quinolone-

50 derived antibiotic with molecular formula $C_{12}H_{12}N_2O_3$ (1-ethyl-7-methyl-4-oxo-[1,8]-

2

naphthyridine-3-carboxylic acid), is causing a major concern due to its release to the environment and frequent presence in surface water and wastewater (Sirtori et al., 2011). Pollice et al. (2012) worked with wastewater containing a NAL concentration of 48 mg L^{-1} in an integrated membrane bioreactor-ozonation system, and Laera et al. (2012) studied different technologies based on membrane bioreactor with diverse oxidation stepts to treat raw wastewater with a NAL concentration of 50 mg L^{-1}. NAL could affect human health through the immune system due to its toxicity and carcinogenicity effects (Patiño et al., 2016; Ibrahim et al., 2002). In this regard, the oral LD_{50} of NAL is 2,040 mg kg^{-1} in rats, and the potential for bioaccumulation has a value of log K_{OW} (n-octanol/water) of 1.59.

In this work, an improved wastewater treatment process called "NIPHO" activated sludge reactor was studied. This technology combines anaerobic, anoxic and aerobic zones within the bioreactor in order to remove nitrogen and phosphorus, as well as carbonaceous compounds, from wastewater (Kim et al., 2013; Leyva-Díaz et al., 2016). This technology requires lower cost, energy and environmental footprint than other technologies for biological nitrogen and phosphorus removal (Park et al., 2010; Lai et al., 2011; Liu et al., 2013). Furthermore, this system has the advantage of stable capacity of simultaneous nutrient removal (Abu-Alhail and Lu, 2014).

Most of current WWTPs were not designed for the abatement of antibiotics. Thus, when wastewater containing antibiotics enters the bioreactor of a wastewater treatment plant (WWTP), they can impact microbial communities of the activated sludge, affecting the biodegradation processes of carbonaceous, nitrogenous or phosphorous compounds (Kümmerer, 2013). To the best of our knowledge, the effect of NAL on the kinetic behavior of heterotrophic and autotrophic biomass in systems based on activated sludge technology has not been reported yet, with very few studies analyzing the influence of

76 emerging pollutants on microbial kinetics, particularly autotrophic kinetics, of

77 biological systems for municipal wastewater treatment (Calero-Díaz et al., 2017; Leyva-

78 Díaz et al., 2017a).

79 In this regard, respirometric method has been used to carry out the kinetic modeling for

80 NIPHO activated sludge system because of its high accuracy and reproducibility

81 (Leyva-Díaz et al., 2013). As a consequence, this will provide further understanding of

82 the influence of NAL on the processes of organic matter and nitrogen removal, which

83 could lead to improved operation of NIPHO activated sludge reactor.

84 The main objective of this study is to analyze the effect of NAL on the heterotrophic

85 and autotrophic biomass of a NIPHO activated sludge bioreactor through the assessment

86 of its kinetic modeling by a respirometric method. This allows to simulate the possible

87 influence of an intrusion of NAL on the heterotrophic and autotrophic microorganisms

88 within the bioreactor and to assess their adaptive capacity through possible

89 modifications in the rates of substrate degradation and net biomass growth. In addition,

90 different mathematical models were developed for the heterotrophic and autotrophic

91 kinetic performance in order to optimize the operational variables, i.e. hydraulic

92 retention time (HRT), biomass concentration as mixed liquor volatile suspended solids

93 (X_{VSS}), temperature (T) and sludge retention time (SRT).

94

95 **2. MATERIALS AND METHODS**

96 **2.1. Description of the NIPHO activated sludge reactor**

97 WWTP of Villapérez is located in the Nora River Basin Sanitation System in the

98 Central Area of Asturias (Spain) and receives wastewater from the surrounding

99 municipalities, including the city of Oviedo. The process line at this plant includes

100 pretreatment, primary settling, biological treatment, secondary settling and tertiary

101 treatment for purification.

102 The biological treatment is carried out through a NIPHO activated sludge reactor, which

103 is fed with municipal wastewater coming from the outlet of the primary settler (Fig. 1).

104 The bioreactor is divided into six zones, i.e. one pre-anoxic zone, one anaerobic zone,

105 two anoxic zones, one facultative zone and one aerobic zone to facilitate the biological

106 nutrient removal (BNR) process. The facultative zone can operate as an oxic or anoxic

107 zone. The aerobic zone provides the optimal conditions for organic substrate removal,

108 nitrification and phosphate assimilation. Internal mixed liquor recirculation consists of a

109 nitrate recirculation from the outlet of the bioreactor to the anoxic zone. The external

110 recirculation is done from the secondary settler to the pre-anoxic zone of the bioreactor

111 to minimize the effect of nitrate in wastewater entering the anaerobic zone, whereas an

112 external recycling is necessary to maintain the working mixed liquor suspended solids

113 (MLSS) concentration inside the bioreactor.

114 **2.2. Operational conditions and activated sludge samples**

115 Activated sludge samples were taken at three different periods, in which the main

116 operation parameters were different: HRT (2.8-3.8 h), X_{VSS} (1,400-1,700 mgVSS L^{-1}), T

117 (12.6-14.8ºC) and SRT (11.0-12.6 day). Table S1 shows the values of these variables

118 for the different periods.

119 Activated sludge samples (each respirometric test requires 2 L of mixed liquor) were

120 collected from the aerobic zone of the NIPHO activated sludge reactor during the steady

121 state of the three operation periods. The different samples of activated sludge were

122 preconditioned by aerating them for 18 h at 20ºC of temperature to achieve endogenous

conditions in which any kind of substrate contained in the sample is consumed (Leyva-Díaz et al., 2013).

2.3. Kinetic study

2.3.1. Experimental system for respirometric assays

After pre-conditioning the sample of activated sludge, one liter of this sample was transferred to the bioreactor of the experimental set-up to carry out the exogenous respirometric assays for heterotrophic and autotrophic biomass in absence of NAL (Fig. S1a). This type of respirometric test was performed by using, firstly, sodium acetate and, subsequently, ammonium chloride under a continuous aeration supplied by an air pump. The bioreactor worked at temperature of 20.0 ± 0.1℃ and stirring rate of 500 rpm to homogenize the mixed liquor. Since pH in the bioreactor was stable throughout the experiments (7.40 ± 0.30), pH control was not necessary. After this respiration test, the endogenous respirometric assay was carried out by leaving without aeration the mixed liquor.

In parallel, both kinds of respiration tests were applied to the remaining liter of sample of activated sludge in presence of NAL. These experiments were initiated when the basis line of DO was accomplished after the addition of NAL solution to get a concentration of 50 mg L^{-1}. The stock solution of NAL was prepared as indicated in Text S1 in the Supplementary Material.

The time course of dissolved oxygen (DO), due to the consumption of substrate sources by the microorganisms, was measured by the oximeter XS, OXY70, with optical O_2 electrode LDO70. The LDO70 probe uses luminescence optical technology for DO measurements in the mixed liquor samples. The oximeter OXY70 has an USB connector for exporting data to PC and DataLink 70 Software.

147   The dynamic oxygen uptake rate (R_S, mgO_2 L^{-1} h^{-1}) was obtained through the derivation

148   of DO depending on the time for the exogenous respirometric experiments (Leyva-Díaz

149   et al., 2017b). In a similar way, the static oxygen uptake rate (OUR, mgO_2 L^{-1} h^{-1}) was

150   calculated through the derivation of DO as a function of the time for the endogenous

151   respiration tests.

152   2.3.2. Estimation of kinetic parameters

153   The kinetic performance for heterotrophic and autotrophic biomass within the NIPHO

154   activated sludge reactor was evaluated under the influence of shock additions of NAL

155   for each one of the three stationary periods of operation.

156   The exogenous respirometric tests included two experiments. The first one was based

157   on the use of sodium acetate at increasing concentrations (50, 80 and 100% of 500 mg

158   L^{-1} stock solution) to determine the kinetic parameters for heterotrophic biomass.

159   Having finished this experiment, the second one is carried out through three additions of

160   ammonium chloride at increasing concentrations (50, 80 and 100% of 150 mg L^{-1} stock

161   solution) to evaluate the kinetic parameters for autotrophic biomass. The preparation of

162   both stock solutions is described in Text S1 in the Supplementary Material. In light of

163   this, when the basis line of DO was achieved, the dynamic oxygen uptake rate for

164   heterotrophic biomass ($R_{S,H}$) was monitored for the additions of carbon source within

165   the operation periods 1, 2 and 3 (Fig. S2). Once the basis line of DO was reestablished,

166   the dynamic oxygen uptake rate for autotrophic biomass ($R_{S,A}$) was registered for the

167   additions of ammonium source in the different operation periods (Fig. S3). The

168   concentrations of heterotrophic and autotrophic biomass, X_H (mgVSS L^{-1}) and X_A

169   (mgVSS L^{-1}), respectively, were calculated by applying the heterotrophic and

170   autotrophic fractions to mixed liquor volatile suspended solids (MLVSS) (Metcalf,

171   2003), which was evaluated from MLSS (APHA, 2012). In this regard, the

172   heterotrophic fractions were 92.51%, 92.58% and 95.47% for the periods 1, 2 and 3,

173   respectively; and the autotrophic fractions resulted in 7.49%, 7.42% and 4.53% for the

174   operation periods 1, 2 and 3, respectively.

175   Regarding the endogenous respirometric test, the evolution of OUR is shown in Fig. S4

176   for the three operation periods.

177   In this way, the exogenous respirometric tests for heterotrophic biomass allowed to

178   evaluate the yield coefficient in absence and presence of NAL ($Y_{H,n/NAL}$ and $Y_{H,NAL}$,

179   respectively), the maximum specific growth rate in absence and presence of NAL

180   ($\mu_{m,H,n/NAL}$ and $\mu_{m,H,NAL}$, respectively) and the half-saturation coefficient for carbon

181   source in absence and presence of NAL ($K_{M,n/NAL}$ and $K_{M,NAL}$, respectively). This kind

182   of experiments for autotrophic biomass provided the assessment of the yield coefficient

183   in absence and presence of NAL ($Y_{A,n/NAL}$ and $Y_{A,NAL}$, respectively), the maximum

184   specific growth rate in absence and presence of NAL ($\mu_{m,A,n/NAL}$ and $\mu_{m,A,NAL}$,

185   respectively) and the half-saturation coefficient for ammonium source in absence and

186   presence of NAL ($K_{NH,n/NAL}$ and $K_{NH,NAL}$, respectively). For its part, the endogenous

187   respiration test enabled the calculation of the decay coefficient for heterotrophic

188   biomass in absence and presence of NAL ($b_{H,n/NAL}$ and $b_{H,NAL}$) and for autotrophic

189   biomass in absence and presence of NAL ($b_{A,n/NAL}$ and $b_{A,NAL}$).

190   Moreover, the degradation rate for carbon source in absence and presence of NAL

191   ($r_{su,H,n/NAL}$ and $r_{su,H,NAL}$, respectively), the degradation rate for ammonium source in

192   absence and presence of NAL ($r_{su,A,n/NAL}$ and $r_{su,A,NAL}$, respectively), the net

193   heterotrophic biomass growth rate in absence and presence of NAL ($r'_{x,H,n/NAL}$ and

194   $r'_{x,H,NAL}$, respectively) and the net autotrophic biomass growth rate in absence and

195   presence of NAL ($r'_{x,A,n/NAL}$ and $r'_{x,A,NAL}$, respectively) were determined.

196   The kinetic parameters for heterotrophic and autotrophic biomass, in absence and

197   presence of NAL, were estimated as indicated in the nine steps described in Text S2 in

198   the Supplementary Material (all equations are included in Table S2). Fig. S1b shows the

199   assessment algorithm for kinetic modeling in absence and presence of NAL.

200   2.3.3. Mathematical modeling and optimization

201   In this research, HRT, X_{VSS}, T and SRT were the independent operational variables.

202   Four models were proposed for the kinetic parameters, i.e. yield coefficient (Y),

203   maximum specific growth rate (μ_m), half-saturation coefficient for substrate source (K_S)

204   and decay coefficient (b), to evaluate the heterotrophic and autotrophic kinetics in

205   absence and presence of NAL. This proposal was based on the mass balances applied to

206   the bioreactor and the relationships established between the operational variables and

207   the kinetic parameters (Leyva-Díaz and Poyatos, 2017).

208   The following models, Eqs. (1)-(4), can be formulated to relate the dependent variables

209   (Y, μ_m, K_S and b) to the independent ones (HRT, X_{VSS}, T and SRT):

210    $$Y = \lambda_{1,H/A} \cdot HRT + \lambda_{2,H/A} \cdot X_{VSS} + \lambda_{3,H/A} \cdot e^{-\frac{\lambda_{4,H/A}}{T}} + \lambda_{5,H/A} \cdot SRT \qquad (1)$$

211    $$\mu_m = \frac{\gamma_{1,H/A}}{HRT} + \frac{\gamma_{2,H/A}}{X_{VSS}} + \gamma_{3,H/A} \cdot e^{-\frac{\gamma_{4,H/A}}{T}} + \frac{\gamma_{5,H/A}}{SRT} \qquad (2)$$

212    $$K_s = \varphi_{1,H/A} \cdot HRT + \varphi_{2,H/A} \cdot X_{VSS} + \varphi_{3,H/A} \cdot e^{-\frac{\varphi_{4,H/A}}{T}} + \varphi_{5,H/A} \cdot SRT \qquad (3)$$

213    $$b = \frac{\alpha_{1,H/A}}{HRT} + \frac{\alpha_{2,H/A}}{X_{VSS}} + \alpha_{3,H/A} \cdot e^{-\frac{\alpha_{4,H/A}}{T}} + \frac{\alpha_{5,H/A}}{SRT} \qquad (4)$$

214   Each of the coefficients $\lambda_{i,H/A}$, $\gamma_{i,H/A}$, $\varphi_{i,H/A}$ and $\alpha_{i,H/A}$ represents the effect of the

215   independent variable on the dependent one. The empirical values of Y, μ_m, K_S and b for

216   heterotrophic and autotrophic biomass in absence and presence of NAL are shown in

217   Table 1. The theoretical values of these parameters were assessed by considering Eqs.

218   (1)-(4) and the best-fit parameter values ($\lambda_{i,H/A}$, $\gamma_{i,H/A}$, $\varphi_{i,H/A}$ and $\alpha_{i,H/A}$) were determined

219   by using the Solver Add-in function of Microsoft Excel. An objective function was

220   defined as the weighted sum of squares of differences between the empirical and

221   theoretical values; this function was minimized to yield the most appropriate parameters

222   for the models formulated (Vining, 2003). The coefficient of determination (R^2) was

223   calculated to verify the goodness of fit, according to Eq. (5):

224    $$R^2 = \frac{\sum_{i=1}^{n}\left(k_i - \hat{k}_i\right)^2}{\sum_{i=1}^{n}(k_i - \bar{k})^2} \qquad (5)$$

225   where k_i indicates the empirical values of the kinetic parameters, $\hat{k}_i$ represents the

226   theoretical values of the kinetic parameters and $\bar{k}$ represent the average values of the

227   empirical kinetic parameters.

228   The models were optimized by considering the operation ranges of HRT (2.8-3.8 h),

229   X_{VSS} (1,400-1,700 mgVSS L^{-1}), T (12.6-14.8ºC) and SRT (11.0-12.6 day) for NIPHO

230   activated sludge reactor. The optimization was performed by the Solver Add-in function

231   of Microsoft Excel. This provided the values of HRT, X_{VSS}, T and SRT that maximized

232   the r´$_X$ for the heterotrophic and autotrophic biomass in absence and presence of NAL.

233   In addition, the optimum values of Y, μ_m, K_S, b and r_{su} were evaluated by considering

234   the optimum operational conditions of HRT, X_{VSS}, T and SRT for the NIPHO activated

235   sludge reactor.

236   **2.4. Statistical analysis**

237   Canoco for Windows v. 4.5 (ScientiaPro, Budapest, Hungary) was applied to carry out a

238   multivariable statistical analysis, which is described in Text S3 in the Supplementary

239   Material.

240

3. RESULTS AND DISCUSSION

3.1. Dynamic and static oxygen uptake rates

3.1.1. Dynamic oxygen uptake rate for heterotrophic biomass ($R_{S,H}$)

Fig. S2 shows the results obtained in the exogenous respirometric tests for heterotrophic biomass of the three operation periods of NIPHO activated sludge reactor. The presence of NAL reduced the duration of the respirometric assays for the three operation periods (Fig. S2a-f). Particularly, the respirometric experiments lasted for 82.7 min, 133.4 min and 83.8 min in presence of NAL, and this time was increased in absence of NAL until 125.0 min, 159.3 min and 105.7 min, respectively, for periods 1, 2 and 3. Thus, the presence of NAL reduced the time required by heterotrophic biomass to degrade the carbon sources. This was in accordance with the research carried out by Leyva-Díaz et al. (2017a) with other emerging pollutant as these authors obtained that the duration of heterotrophic experiments was diminished in presence of bisphenol A at similar temperature (12.1ºC) in an MBR system. As a whole, the maximum values for R_S increased with the addition of NAL in periods 1 and 2, and these values were similar in the third period (Fig. S2). This could be due to the fact that periods 1 and 2 worked at the most favorable operation conditions of X_{VSS} (1,600 and 1,700 mgVSS L^{-1}) and T (13.7 and 14.8ºC) compared with the third period, which compensated the effect of NAL.

In spite of its most advantageous working conditions (X_{VSS}=1,700 mgVSS L^{-1} and T=14.8ºC), the experiments corresponding to the second period had the highest duration in absence and presence of NAL (159.3 min and 133.4 min, respectively). This was probably due to the lowest value of SRT (11.0 day), which minimised the effect of X_{VSS} and T. Nevertheless, the duration of the respirometric assay was the lowest in the third

265   period in absence of NAL (105.7 min) even though the operation conditions regarding

266   X_{VSS} and T were the most unfavorable (X_{VSS}=1,400 mg L^{-1} and T=12.6ºC), which stated

267   the highest effect of HRT in this period (HRT=3.8 h). Under the presence of NAL, the

268   lowest duration of the respirometric tests corresponded to the first and third periods with

269   values of 82.7 min and 83.8 min, respectively. The effect of HRT prevailed over the

270   other operation conditions in the third period, as occurred in absence of NAL. In the

271   case of the first period, the value of SRT (12.6 day) was the most favorable and exerted

272   a higher effect than the rest of variables.

273   3.1.2. Dynamic oxygen uptake rate for autotrophic biomass ($R_{S,A}$)

274   The exogenous respiration experiments for autotrophic biomass within the NIPHO

275   activated sludge reactor are depicted in Fig. S3 for each of the operation periods. In this

276   case, the presence of NAL increased the duration of the experiments in periods 1 and 2

277   (Fig. S3a-d), which implied a higher time required by autotrophic biomass to degrade

278   the ammonium source. Specifically, the respirometric tests lasted for 90.0 min and

279   111.5 min in absence of NAL, and 112.8 min and 186.7 min in presence of NAL for

280   periods 1 and 2, respectively. However, a reverse trend was recorded in period 3, i.e. the

281   experiment extended for 94.7 min in absence of NAL and 82.1 min in presence of NAL.

282   This could be due to the effect of HRT, which was the highest in the third period (3.8

283   h). In general, the maximum values for R_S decreased with the addition of NAL in all

284   operation periods. This was probably due to the higher influence of NAL on the

285   autotrophic biomass than the effect caused by the most favorable operation variables in

286   the first and second periods (X_{VSS} and T), and in the third period (HRT).

287   The duration of autotrophic experiments was also the highest in the second period in

288   absence and presence of NAL, as occurred in heterotrophic experiments. This

289   corroborated the fact that the influence of SRT (11.0 day) compensated the most

290 favorable operation conditions of X_{VSS} and T. However, in this case, the duration of the

291 respirometric test was the lowest in the first period in absence of NAL (90.0 min), in

292 which the value of SRT was the most advantageous (12.6 day). In presence of NAL, the

293 effect of HRT (3.8 h) prevailed over X_{VSS} and T in the third period, which had the

294 shortest duration (82.1 min). Thus, for autotrophic experiments, SRT exerted a higher

295 influence on autotrophic bacteria in period 1 in absence of NAL, and HRT had a higher

296 effect on this kind of biomass in period 3 in presence of NAL.

297 3.1.3. Static oxygen uptake rate (OUR)

298 Fig. S4 depicts the endogenous respirometric assays for the three operation periods of

299 the NIPHO activated sludge reactor. It should be highlighted that the presence of NAL

300 lessened the maximum value of OUR, which corresponded to OUR_{end}, in the three

301 operation periods. In particular, OUR_{end} was diminished from 8.220 to 6.230 mgO_2 L^{-1}

302 h^{-1} in the first period, from 7.321 to 5.942 mgO_2 L^{-1} h^{-1} in the second period, and from

303 4.892 to 3.934 mgO_2 L^{-1} h^{-1} in the third period. This trend was also observed in the

304 research carried out by Leyva-Díaz et al. (2017a) with bisphenol A as emerging

305 pollutant.

306 **3.2. Modeling and optimization of heterotrophic kinetics**

307 3.2.1. Kinetic parameters

308 Table 1 shows the kinetic parameters for heterotrophic and autotrophic biomass in

309 absence and presence of NAL for the three operation stages.

310 The values of Y_H were lower in presence of NAL ($Y_{H,NAL}$) than in absence of NAL

311 ($Y_{H,n/NAL}$), with reductions of 33.49%, 12.29% and 9.46% for periods 1, 2 and 3,

312 respectively. This resulted in a lower amount of heterotrophic biomass produced per

313 carbonaceous substrate oxidized in presence of NAL.

314   On the contrary, the values of $\mu_{m,H}$ increased in presence of NAL ($\mu_{m,H,NAL}$) if compared

315   with those values in absence of NAL ($\mu_{m,H,n/NAL}$). The values of $\mu_{m,H,NAL}$ surpassed

316    $\mu_{m,H,n/NAL}$ in 43.33%, 52.46% and 17.65% for periods 1, 2 and 3, respectively, implying

317   less time to oxidize carbon source by heterotrophic bacteria in presence of NAL. The

318   same trend could be observed for K_M, with higher values in presence of NAL (Table 1).

319   Similar results were obtained by Calero-Díaz et al. (2017), who evaluated the effect of a

320   combination of pharmaceuticals on the heterotrophic kinetics of an MBR system.

321   Among the three pharmaceuticals analyzed, they worked with other antibiotic

322   (ciprofloxacin) and obtained that Y_H was reduced, and $\mu_{m,H}$ and K_M were increased in

323   presence of these emerging pollutants.

324   Regarding the values of b_H, they were higher in absence of NAL ($b_{H,n/NAL}$) than in

325   presence of NAL ($b_{H,NAL}$), with reduction rates of 36.36%, 30.29% and 23.77% for

326   periods 1, 2 and 3, respectively, in presence of NAL. Thus, the presence of NAL

327   diminished the heterotrophic decay rate, that is, the quantity of heterotrophic biomass

328   oxidized per day. The values of OUR_{end} (Fig. S4) supported these results as they also

329   decreased in presence of NAL. This result was also obtained by Leyva-Díaz et al.

330   (2017a) studying the effect of bisphenol A within an MBR system, although the

331   reduction percentages were lower (3.91-9.17%).

332   3.2.2. Degradation rate for carbon source ($r_{su,H}$) and net biomass growth rate ($r´_{x,H}$)

333   Fig. 2a shows the values of $r_{su,H}$ in absence and presence of NAL for the three operation

334   stages. It must be pointed out that the $r_{su,H}$ increased in presence of NAL in percentages

335   of 88.33% for period 1, 62.74% for period 2, and 23.21% for period 3. The reason could

336   be that the presence of NAL imposed a physiological stress on heterotrophic bacteria

337   and heterotrophs possibly counteracted the situation by increasing the $r_{su,H}$ in order to

14

338 facilitate their acclimatization. Moreover, according to Bouki et al. (2013), this could be

339 explained by the fact that environmental conditions in WWTPs are suitable for the

340 acquisition and spread of antibiotic resistant bacteria, which may transfer resistance

341 genes to resident bacteria. In light of this, Zhang et al. (2015) first time identified and

342 characterized antibiotic-resistant heterotrophic bacteria from different WWTPs.

343 Vasiliadou et al. (2018) also studied the effect of pharmaceutical compounds on mixed

344 culture from activated sludge using respirometric method and obtained an adaptation of

345 microorganisms that was based on modifications of microbial community, increasing its

346 resistance to pharmaceuticals. In this way, the degradation of carbon source occurred

347 faster in presence of NAL than in absence of this antibiotic at a biodegradation rate of

348 NAL of $1.73\pm0.14\%$ during heterotrophic test. The highest values of $r_{su,H}$ corresponded

349 to heterotrophic biomass from the second period in absence and presence of NAL

350 (25.88 and 42.12 mgO_2 L^{-1} h^{-1}, respectively), which could be due to the operation at the

351 highest values of X_{VSS} (1,700 $mgVSS$ L^{-1}) and T (14.8°C) (Table S1). Fig. 2b represents

352 the values of $r´_{x,H}$ in absence and presence of NAL. The trend was similar to that

353 obtained for $r_{su,H}$, with an increase of $r´_{x,H}$ in presence of NAL. Heterotrophic biomass

354 subjected to the operation conditions of period 2 had the highest $r´_{x,H}$ in presence of

355 NAL (6.73 $mgVSS$ L^{-1} h^{-1}), which was probably caused by the most favorable operation

356 conditions of this period regarding X_{VSS} and T, as happened previously for $r_{su,H}$. In

357 relation to the operation in absence of NAL, heterotrophic biomass corresponding to

358 period 3 showed the highest $r´_{x,H}$ (2.91 $mgVSS$ L^{-1} h^{-1}), which could be explained by the

359 highest effect of HRT (3.8 h).

360 3.2.3. Modeling and optimization

361 Regarding the mathematical models to fit the heterotrophic kinetics depending on HRT,

362 X_{VSS}, T and SRT in absence and presence of NAL, the values of R^2 fluctuated between

363   0.97085 and 0.99975 (Table 2). This confirmed that the proposed mathematical models

364   had a high goodness of fit for the kinetic parameters characterizing the heterotrophic

365   bacteria within the NIPHO activated sludge reactor. Moreover, Fig. 3a-b shows the

366   results of the multivariable statistical analysis for heterotrophic kinetic modeling in

367   absence and presence of NAL.

368   In light of this, in absence of NAL (Fig. 3a), $Y_{H,n/NAL}$ showed a positive correlation with

369   SRT and a strongly negative correlation with HRT, which was supported by the fitting

370   parameters $\lambda_{5,H}$ (0.02416) and $\lambda_{1,H}$ (-0.00377), respectively. A similar trend was

371   observed for $\mu_{m,H,n/NAL}$ and $b_{H,n/NAL}$, although the effect of SRT on these parameters was

372   slightly lower and the influence of X_{VSS} and T was slightly higher than for $Y_{H,n/NAL}$.

373   This was corroborated by the coefficients $\gamma_{i,H}$ and $\alpha_{i,H}$ in absence of NAL. In relation to

374    $K_{M,n/NAL}$, it was directly proportional to X_{VSS} and T, as indicated by the triplot diagram

375   and the fitting parameters $\varphi_{2,H}$ (0.00208), $\varphi_{3,H}$ (0.01107) and $\varphi_{4,H}$ (0.00002). However, it

376   was negatively correlated with SRT ($\varphi_{5,H}$=-0.31326) and HRT had almost no influence

377   on it as the angles between these vectors are approximately 90º. Furthermore, $r_{su,H,n/NAL}$

378   had a strongly positive correlation with X_{VSS} and T, and $r´_{x,H,n/NAL}$ was positively

379   correlated with HRT (Fig. 3a). This confirmed the previous results in which

380   heterotrophic biomass from period 2 worked at the most favorable operation conditions

381   of X_{VSS} and T and showed the highest values for $r_{su,H,n/NAL}$, and heterotrophic biomass

382   from period 3 operated at the greatest HRT and presented the highest value of $r´_{x,H,n/NAL}$.

383   The optimum operational conditions in terms of HRT, X_{VSS}, T and SRT were 3.8 h,

384   1,566 mgVSS L^{-1}, 12.6ºC and 12.6 day, respectively (Table 2), which allowed to obtain

385   the optimum values of 23.96 mgO$_2$ L^{-1} h^{-1} and 3.93 mgVSS L^{-1} h^{-1} for $r_{su,H,n/NAL}$ and

386    $r´_{x,H,n/NAL}$, respectively.

387   The presence of NAL modified the results obtained in absence of NAL, as shown in

388   Fig. 3b. In this way, $Y_{H,NAL}$ had a slightly positive correlation with HRT and SRT. Its

389   correlation with X_{VSS} and T was strongly negative, according to the values $\lambda_{i,H}$ from

390   Table 2. A similar trend was observed for $\mu_{m,H,NAL}$ and $b_{H,NAL}$, although the effect of

391   SRT on these parameters was slightly higher and the influence of HRT was slightly

392   lower than for $Y_{H,NAL}$. This was confirmed by the coefficients $\gamma_{i,H}$ and $\alpha_{i,H}$ in presence of

393   NAL. Regarding the $K_{M,NAL}$, it had a direct proportionality with X_{VSS} and T, as

394   demonstrated by the fitting parameters $\varphi_{2,H}$ (0.00900), $\varphi_{3,H}$ (-0.14500) and $\varphi_{4,H}$ (-

395   0.00019). Nevertheless, it was negatively correlated with HRT ($\varphi_{1,H}$=-2.02909), and

396   SRT did not practically affect it. In presence of NAL, SRT replaced X_{VSS} and T, and

397   was the operation variable with the highest influence on $r_{su,H,NAL}$, and HRT continued to

398   have the greatest effect on $r´_{x,H,NAL}$ in presence of NAL (Fig. 3b). The optimum values

399   corresponding to the operational variables were 2.8 h for HRT, 1,566 mgVSS L^{-1} for

400   X_{VSS}, 14.8ºC for T and 11.0 day for SRT, which implied optimum values for $r_{su,H,NAL}$

401   and $r´_{x,H,NAL}$ that practically doubled those obtained in absence of NAL (54.52 mgO$_2$ L^{-1}

402   h^{-1} and 6.68 mgVSS L^{-1} h^{-1}, respectively).

403   **3.3. Modeling and optimization of autotrophic kinetics**

404   3.3.1. Kinetic parameters

405   The autotrophic kinetic parameters in absence and presence of NAL are shown in Table

406   1 for the different operation periods.

407   The values of Y_A were higher in presence of NAL ($Y_{A,NAL}$) than in absence of NAL

408   ($Y_{A,n/NAL}$), with increases of 1.20%, 18.17% and 26.67% for periods 1, 2 and 3,

409   respectively. This implied a higher amount of autotrophic biomass produced per

410   nitrogenous substrate oxidized in presence of NAL.

411   However, the values of $\mu_{m,A}$ decreased in presence of NAL ($\mu_{m,A,NAL}$) in relation to

412   those values in absence of NAL ($\mu_{m,A,n/NAL}$), with reduction percentages of 63.26%,

413   59.27% and 64.71% for periods 1, 2 and 3, respectively. Thus, the time required to

414   oxidize ammonium source by autotrophic bacteria was higher in presence of NAL than

415   in absence of this antibiotic. The same trend was obtained for K_{NH}, with lower values in

416   presence of NAL.

417   In relation to the values of b_A, they were higher in absence of NAL ($b_{A,n/NAL}$) than in

418   presence of NAL ($b_{A,NAL}$), as occurred for b_H. In this case, the presence of NAL also

419   lessened the autotrophic decay rate, that is, the quantity of autotrophic biomass oxidized

420   per day. In particular, the reduction percentages were 38.67%, 30.27% and 20.74% for

421   periods 1, 2 and 3, respectively. This was confirmed by the decrease of OUR_{end} in

422   presence of NAL, as shown in Fig. S4. It should be highlighted that the autotrophic

423   decay rate was lower in period 1 in relation to periods 2 and 3, which could be due to its

424   higher SRT (12.6 day).

425   3.3.2. Degradation rate for ammonium source ($r_{su,A}$) and net biomass growth rate ($r'_{x,A}$)

426   Fig. 2c depicts the values of $r_{su,A}$ in absence and presence of NAL for the different

427   operation periods. The presence of NAL reduced the $r_{su,A}$ in 61.99% for the first period,

428   64.29% for the second period and 67.70% for the third period, which implied that the

429   degradation of ammonium source occurred slower in presence of NAL at a

430   biodegradation rate of NAL of 1.45±0.12% during autotrophic test. This trend was

431   opposed to that observed for heterotrophic biomass. The highest values of $r_{su,A}$ were

432   registered for autotrophic biomass from period 2 in absence and presence of NAL

433   (36.78 mgN L^{-1} h^{-1} and 13.14 mgN L^{-1} h^{-1}, respectively), which could be caused by the

434   working at the most favorable operation conditions of X_{VSS} and T (1,700 mgVSS L^{-1}

435   and 14.8ºC, respectively). Fig. 2d shows the values of $r'_{x,A}$ in absence and presence of

436   NAL. For $r'_{x,A}$, the presence of NAL also reduced its value for periods 1, 2 and 3, as

437   occurred for $r_{su,A}$. Autotrophic biomass from the third period showed values of $r'_{x,A}$

438   slightly higher than those obtained from the first and second periods both in absence of

439   NAL and in presence of this antibiotic (25.37 mgVSS L^{-1} h^{-1} and 10.29 mgVSS L^{-1} h^{-1},

440   respectively). This could be explained by the highest value of HRT (3.8 h)

441   characterizing this operation period.

442   If the values of $r_{su,A}$ and $r'_{x,A}$ are compared with the corresponding values of $r_{su,H}$ and

443    $r'_{x,H}$, it is necessary to indicate that NAL exerted a negative effect on autotrophic

444   biomass in relation to the influence observed on heterotrophic biomass within the

445   NIPHO activated sludge reactor.

446   In light of this, Kraigher et al. (2008) studied the influence of pharmaceuticals

447   (ibuprofen, naproxen, ketoprofen, diclofenac and clofibric acid) on the structure of

448   activated sludge bacterial communities from a bioreactor that worked at a HRT of 48 h

449   and at a SRT of over 100 days. They obtained that the genus *Nitrospira*, which

450   represented 8% of the total community, was only found in the bioreactor without

451   pharmaceuticals. This indicated that nitrite-oxidizing bacteria, which play a key role for

452   the second stage of nitrification in WWTPs, were affected in presence of

453   pharmaceuticals. Dokianakis et al. (2004) obtained similar results to those shown by

454   Kraigher et al. (2008). This was in accordance with the partial inhibitory effect of NAL

455   on autotrophic bacteria in the current research.

456   3.3.3. Modeling and optimization

457   Mathematical modeling fitting the autotrophic kinetics depending on HRT, X_{VSS}, T and

458   SRT in absence and presence of NAL had a higher goodness of fit than that for

459   heterotrophic kinetics, with values for R^2 varying between 0.99913 and 0.99997 (Table

460   2). In addition, Fig. 3c-d depicts the results of the multivariable statistical analysis for

461 autotrophic kinetic modeling in absence and presence of NAL. In absence of NAL (Fig.

462 3c), $Y_{A,n/NAL}$ exhibited a positive correlation with X_{VSS} and T, whereas it had a negative

463 correlation with HRT. The influence of SRT was slightly low, as the angle between the

464 vectors was almost of 90°. In the case of $\mu_{m,A,n/NAL}$, it was positively correlated with

465 HRT, X_{VSS} and T, as indicated by the values $\gamma_{1,A}$, $\gamma_{2,A}$, $\gamma_{3,A}$ and $\gamma_{4,A}$, while it was

466 strongly negative correlated with SRT ($\gamma_{5,A}$). Regarding $K_{NH,n/NAL}$, it had a positive

467 correlation with HRT, which was supported by the fitting parameter $\varphi_{1,A}$ (0.11956). The

468 influence of X_{VSS} and T on this kinetic parameter was negligible, as shown the angles

469 between the vectors (close to 90°) and the low values of $\varphi_{2,A}$, $\varphi_{3,A}$ and $\varphi_{4,A}$. In relation to

470 the influence of SRT, the trend was similar to that observed for $\mu_{m,A,n/NAL}$. The

471 correlation between $b_{A,n/NAL}$ and the operational conditions X_{VSS} and T was strongly

472 positive. This was corroborated by the coefficients $\alpha_{2,A}$ (0.56121), $\alpha_{3,A}$ (0.23255) and

473 $\alpha_{4,A}$ (-0.14763). However, $b_{A,n/NAL}$ had a negative correlation with SRT ($\alpha_{5,A}$=-0.64990).

474 The angle formed between the vectors corresponding to $b_{A,n/NAL}$ and HRT was 90°,

475 which meant that this variable did not practically influence on this kinetic parameter.

476 Moreover, $r_{su,A,n/NAL}$ had a positive correlation with X_{VSS} and T, and $r'_{x,A,n/NAL}$ showed a

477 positive correlation with SRT (Fig. 3c). This corroborated the previous results in which

478 autotrophic biomass from period 2 had the highest values for $r_{su,A,n/NAL}$ at the most

479 favorable operation conditions of X_{VSS} and T. The optimum values for $r_{su,A,n/NAL}$ and

480 $r'_{x,A,n/NAL}$ were 69.21 mgN L^{-1} h^{-1} and 55.02 mgVSS L^{-1} h^{-1}, respectively, at HRT of 3.8

481 h, X_{VSS} of 125 mgVSS L^{-1}, T of 12.6°C and SRT of 12.6 day (Table 2).

482 Fig. 3d shows the differences generated as a consequence of the effect of NAL on

483 autotrophic biomass in relation to the absence of NAL. In this regard, $Y_{A,NAL}$ showed a

484 slightly positive correlation with HRT and SRT, and it was inversely proportional to

485 X_{VSS} and T, as supported by the fitting parameters $\lambda_{i,A}$. In general, a similar trend was

486 observed for $\mu_{m,A,NAL}$, $K_{NH,NAL}$ and $b_{A,NAL}$, with a positive correlation regarding X_{VSS}

487 and T, a slightly positive correlation with HRT, and a strongly negative correlation with

488 SRT, as indicated by the fitting parameters $\gamma_{i,A}$, $\varphi_{i,A}$ and $\alpha_{i,A}$, respectively. In presence of

489 NAL, X_{VSS} and T continued to have influence on $r_{su,A,NAL}$ and their effect was higher

490 than in absence of NAL due to the lower angles between the vectors corresponding to

491 X_{VSS}, T and $r_{su,A,NAL}$. Regarding $r´_{x,A,NAL}$, it was directly proportional to SRT, as

492 occurred in absence of NAL, and had also a slightly direct proportionality with HRT

493 (Fig. 3d). This confirmed the previous results in which autotrophic biomass from the

494 third period had a slightly higher value for $r´_{x,A,NAL}$ than in the rest of operation periods

495 due to its operation at the highest HRT (3.8 h). In this case, the optimum values for the

496 operational conditions were identical to those obtained in absence of NAL (HRT=3.8 h,

497 X_{VSS}=125 mgVSS L^{-1}, T=12.6ºC and SRT=12.6 day). This implied optimum values for

498 $r_{su,A,NAL}$ and $r´_{x,A,NAL}$ of 22.02 mgN L^{-1} h^{-1} and 20.23 mgVSS L^{-1} h^{-1}, respectively (Table

499 2).

500 It should be highlighted that the different models were optimized for the operation

501 ranges of HRT (2.8-3.8 h), X_{VSS} (1,400-1,700 mgVSS L^{-1}), T (12.6-14.8ºC) and SRT

502 (11.0-12.6 day) in the NIPHO activated sludge reactor. Thus, this methodology provides

503 a preview to achieve the optimum operation conditions for desirable responses in

504 relation to the biological processes of organic matter and nitrogen removal in absence

505 and presence of NAL, and to carry out a more precise control of these processes. To the

506 best of our knowledge, obtaining mixed liquor samples from a real WWTP at three

507 different operation conditions is novel for the kinetic modeling and optimization of

508 biological processes.

509

510

4. CONCLUSIONS

The following conclusions were drawn from the kinetic modeling and optimization of a NIPHO activated sludge reactor treating municipal wastewater under the influence of shock additions of nalidixic acid (NAL) for three operation periods, highlighting the novelty of obtaining activated sludge samples from a real WWTP at three different operation conditions:

- The degradation rate for carbon source ($r_{su,H}$) increased in presence of NAL, which implied a faster consumption of carbon source than in absence of NAL. However, degradation rate for ammonium source ($r_{su,A}$) diminished in presence of NAL, which meant a slower degradation of nitrogen source than in absence of NAL. Similar trends were observed for the net heterotrophic biomass growth rate ($r'_{x,H}$) and net autotrophic biomass growth rate ($r'_{x,A}$). Thus, the heterotrophic biomass of the NIPHO activated sludge reactor was not inhibited by the presence of NAL, showing an adaptive capacity to improve $r_{su,H}$ and $r'_{x,H}$. However, the autotrophic biomass was negatively affected by the presence of NAL, reducing the values of $r_{su,A}$ and $r'_{x,A}$.

- Heterotrophic and autotrophic kinetic performance in terms of yield coefficient (Y), maximum specific growth rate (μ_m), half-saturation coefficient for substrate source (K_S) and decay coefficient (b) could be modeled depending on HRT, XVSS, T and SRT, according to the following functions:

$$Y = \lambda_{1,H/A} \cdot HRT + \lambda_{2,H/A} \cdot X_{VSS} + \lambda_{3,H/A} \cdot e^{-\frac{\lambda_{4,H/A}}{T}} + \lambda_{5,H/A} \cdot SRT$$

$$\mu_m = \frac{\gamma_{1,H/A}}{HRT} + \frac{\gamma_{2,H/A}}{X_{VSS}} + \gamma_{3,H/A} \cdot e^{-\frac{\gamma_{4,H/A}}{T}} + \frac{\gamma_{5,H/A}}{SRT}$$

$$K_s = \varphi_{1,H/A} \cdot HRT + \varphi_{2,H/A} \cdot X_{VSS} + \varphi_{3,H/A} \cdot e^{-\frac{\varphi_{4,H/A}}{T}} + \varphi_{5,H/A} \cdot SRT$$

$$b = \frac{\alpha_{1,H/A}}{HRT} + \frac{\alpha_{2,H/A}}{X_{VSS}} + \alpha_{3,H/A} \cdot e^{-\frac{\alpha_{4,H/A}}{T}} + \frac{\alpha_{5,H/A}}{SRT}$$

534 • The variables with the highest influence on $r_{su,H}$ and $r_{su,A}$ were the biomass

535 concentration (X_{VSS}) and temperature (T), with the exception for $r_{su,H}$ in presence of

536 NAL that was more affected by sludge retention time (SRT). Hydraulic retention

537 time (HRT) was the variable with the greatest effect on $r'_{x,H}$, and SRT had the

538 highest influence on $r'_{x,A}$ in absence and presence of NAL.

539

540 **Acknowledgements**

544

545 **Appendix. Supplementary material**

546 Supplementary data associated with this article can be found, in the online version, at …

Nomenclature

b	decay coefficient
$b_{A,NAL}$	decay coefficient for autotrophic biomass in presence of NAL
$b_{A,n/NAL}$	decay coefficient for autotrophic biomass in absence of NAL
$b_{H,NAL}$	decay coefficient for heterotrophic biomass in presence of NAL
$b_{H,n/NAL}$	decay coefficient for heterotrophic biomass in absence of NAL
BNR	biological nutrient removal
COD	chemical oxygen demand
DCA	detrended correspondence analysis
DO	dissolved oxygen
HRT	hydraulic retention time
$K_{M,NAL}$	half-saturation coefficient for carbon source in presence of NAL
$K_{M,n/NAL}$	half-saturation coefficient for carbon source in absence of NAL
$K_{NH,NAL}$	half-saturation coefficient for ammonium source in presence of NAL
$K_{NH,n/NAL}$	half-saturation coefficient for ammonium source in absence of NAL
K_S	half-saturation coefficient for substrate source
MLSS	mixed liquor suspended solids
NAL	nalidixic acid
OUR	static oxygen uptake rate

RDA	redundancy analysis
r_{su}	substrate degradation rate
$r_{su,A,NAL}$	degradation rate for ammonium source in presence of NAL
$r_{su,A,n/NAL}$	degradation rate for ammonium source in absence of NAL
$r_{su,H,NAL}$	degradation rate for carbon source in presence of NAL
$r_{su,H,n/NAL}$	degradation rate for carbon source in absence of NAL
r'_{x}	net biomass growth rate
$r'_{x,A,NAL}$	net autotrophic biomass growth rate in presence of NAL
$r'_{x,A,n/NAL}$	net autotrophic biomass growth rate in absence of NAL
$r'_{x,H,NAL}$	net heterotrophic biomass growth rate in presence of NAL
$r'_{x,H,n/NAL}$	net heterotrophic biomass growth rate in absence of NAL
R_{S}	dynamic oxygen uptake rate
$R_{S,A}$	dynamic oxygen uptake rate for autotrophic biomass
$R_{S,H}$	dynamic oxygen uptake rate for heterotrophic biomass
SRT	sludge retention time
T	temperature
WWTP	wastewater treatment plant
X_{VSS}	biomass concentration as mixed liquor volatile suspended solids
X_{A}	concentration of autotrophic biomass
X_{H}	concentration of heterotrophic biomass
X_{T}	total biomass concentration
Y	yield coefficient
$Y_{A,NAL}$	yield coefficient for autotrophic biomass in presence of NAL
$Y_{A,n/NAL}$	yield coefficient for autotrophic biomass in absence of NAL
$Y_{H,NAL}$	yield coefficient for heterotrophic biomass in presence of NAL
$Y_{H,n/NAL}$	yield coefficient for heterotrophic biomass in absence of NAL

Greek symbols

λ	fitting parameter for yield coefficient
γ	fitting parameter for maximum specific growth rate
φ	fitting parameter for half-saturation coefficient for substrate source
α	fitting parameter for decay coefficient
μ_{m}	maximum specific growth rate
$\mu_{m,A,NAL}$	maximum specific growth rate for autotrophic biomass in presence of NAL
$\mu_{m,A,n/NAL}$	maximum specific growth rate for autotrophic biomass in absence of NAL
$\mu_{m,H,NAL}$	maximum specific growth rate for heterotrophic biomass in presence of NAL
$\mu_{m,H,n/NAL}$	maximum specific growth rate for heterotrophic biomass in absence of NAL

547

References

549 Abu-Alhail, S., Lu, X.W., 2014. Experimental investigation and modeling of innovative

550 five-tank anaerobic-anoxic/oxic process. Appl. Math. Model. 38 (1), 278–290.

551 APHA, 2012. Standard Methods for the Examination of Water and Wastewater, 22nd

552 ed. American Public Health Association, Washington DC.

553 Bouki, C., Venieri, D., Diamadopoulos, E., 2013. Detection and fate of antibiotic

554 resistant bacteria in wastewater treatment plants: a review. Ecotox. Environ. Safe. 91,

555 1–9.

556 Calero-Díaz, G., Monteoliva-García, A., Leyva-Díaz, J.C., López-López, C., Martín-

557 Pascual, J., Torres, J.C., Poyatos, J.M., 2017. Impact of ciprofloxacin, carbamazepine

558 and ibuprofen on a membrane bioreactor system: Kinetic study and biodegradation

559 capacity. J. Chem. Technol. Biot. 92, 2944–2951.

560 Dokianakis, S.N., Kornaros, M.E., Lyberatos, G., 2004. On the effect of

561 pharmaceuticals on bacterial nitrite oxidation. Water Sci. Technol. 50 (5), 341-346.

562 Gelbrand, H., Miller-Petrie, M., Pant, S., Gandra, S., Levinson, J., Barter, D., White, A.,

563 Laxminarayan, R., Ganguly, N., Kariuki, S., 2015. The State of the World's Antibiotics

564 2015. Wound Healing S. Afr. 8 (2), 30–34.

565 Huang, C.H., Renew, J.E., Smeby, K.L., Pinkerston, K., Sedlak, D.L., 2001.

566 Assessment of potential antibiotic contaminants in water and preliminary occurrence

567 analysis. Water Resour. Update 120, 30-40.

568 Ibrahim, M.S., Shehatta, I.S., Sultan, M.R., 2002. Cathodic adsorptive stripping

569 voltammetric determination of nalidixic acid in pharmaceuticals, human urine and

570 serum. Talanta 56, 471–479.

571 Kim, B.C., Kim, S., Shin, T., Kim, H., Sang, B.I., 2013. Comparison of the bacterial

572 communities in anaerobic, anoxic, and oxic chambers of a pilot A^2O process using

573 pyrosequencing analysis. Curr. Microbiol. 66 (6), 555–565.

574 Kraigher, B., Kosjek, T., Heath, E., Kompare, B., Mandic-Mulec, I., 2008. Influence of

575 pharmaceutical residues on the structure of activated sludge bacterial communities in

576 wastewater treatment bioreactors. Water Res. 42, 4578–4588.

577 Kummerer, K., 2009. Antibiotics in the aquatic environment: a review e part II.

578 Chemosphere 75, 435-441.

579 Kümmerer, K., 2013. Pharmaceuticals in the Environment: sources, fate, effects and

580 risks, Springer, Berlin.

581 Laera, G., Cassano, D., Lopez, A., Pinto, A., Pollice, A., Ricco, G., Mascolo, G., 2012.

582 Removal of Organics and Degradation Products from Industrial Wastewater by a

583 Membrane Bioreactor Integrated with Ozone or UV/H2O2 Treatment. Environ. Sci.

584 Technol. 46, 1010−1018.

585 Lai, T.M., Dang, H.V., Nguyen, D.D., Yim, S., Hur, J., 2011. Wastewater treatment

586 using a modified A^2O process based on fiber polypropylene media. J. Environ. Sci.

587 Health A Tox. Hazard. Subst. Environ. Eng. 46 (10), 1068-1074.

588 Lekunberri, I., Villagrasa, M., Balcázar, J.L., Borrego, C.M., 2017. Contribution of

589 bacteriophage and plasmid DNA to the mobilization of antibiotic resistance genes in a

590 river receiving treated wastewater discharges. Sci. Total Environ. 601–602, 206–209.

591 Leyva-Díaz, J.C., Calderón, K., Rodríguez, F.A., González-López, J., Hontoria, E.,

592 Poyatos, J.M., 2013. Comparative kinetic study between moving bed biofilm reactor-

593 membrane bioreactor and membrane bioreactor systems and their influence on organic

594 matter and nutrients removal. Biochem. Eng. J. 77, 28–40.

595 Leyva-Díaz, J.C., Muñío, M.M., González-López, J., Poyatos, J.M., 2016.

596 Anaerobic/anoxic/oxic configuration in hybrid moving bed biofilm reactor-membrane

597 bioreactor for nutrient removal from municipal wastewater. Ecol. Eng. 91, 449-458.

598 Leyva-Díaz, J.C., Poyatos, J.M., 2017. Modeling and optimization of membrane

599 bioreactors and moving bed biofilm reactor-membrane bioreactors. Chem. Eng.

600 Technol. 40 (9), 1726-1735.

601 Leyva-Díaz, J.C., Calero-Díaz, G., López-López, C., Martín-Pascual, J., Torres, J.C.,

602 Poyatos, J.M., 2017a. Kinetic study of the effect of bisphenol A on the rates of organic

603 matter removal, decay and biomass generation in a membrane bioreactor. Biochem.

604 Eng. J. 128, 45–53.

605 Leyva-Díaz, J.C., Poyatos, J.M., Barghini, P., Gorrasi, S., Fenice, M., 2017b. Kinetic

606 modeling of Shewanella baltica KB30 growth on different substrates through

607 respirometry. Microb. Cell Fact. 16, 189.

608 Liu, Y., Hu, J., Xu, B., He, J., Gao, P., Liu, K., Xue, G., Ognier, S., 2013. Isolation and

609 identification of an iopromide-degrading strain and its application in an A^2O system.

610 Bioresour. Technol. 134, 36-42.

611 Metcalf, E., 2003. Wastewater Engineering Treatment and Reuse, Mc Graw Hill, United

612 Kingdom.

613 Mojica, E.R.E., Aga, D.S., 2011. Antibiotics pollution in soil and water: potential

614 ecological and human health issues, in: J.O. Nriagu (Ed.), Encyclopedia of

615 Environmental Health, Elsevier, Burlington, pp. 97–110.

616 Park, S., Choi, K., 2008. Hazard assessment of commonly used agricultural antibiotics

617 on aquatic ecosystems. Ecotoxicology 17, 526–538.

618 Park, H.O., Oh, S., Bade, R., Shin, W.S., 2010. Application of A^{2}O moving-bed biofilm

619 reactors for textile dyeing wastewater treatment. Korean J. Chem. Eng. 27 (3), 893-899.

620 Patiño, Y., Díez, E., Ordóñez, S., 2016. Pre-concentration of nalidixic acid through

621 adsorption-desorption cycles: Adsorbent selection and modeling. Chem. Eng. J. 283,

622 486-494.

623 Pollice, A., Laera, G., Cassano, D., Diomede, S., Pinto, A., Lopez, A., Mascolo, G.,

624 2012. Removal of nalidixic acid and its degradation products by an integrated MBR-

625 ozonation system. J. Hazard. Mater. 203–204, 46–52.

626 Servais, P., Passerat, J., 2009. Antimicrobial resistance of fecal bacteria in waters of the

627 Seine river watershed (France). Sci. Total Environ. 408, 365–372.

628 Sirtori, C., Zapata, A., Gernjak, W., Malato, S., Lopez, A., Agüera, A., 2011. Solar

629 photo-Fenton degradation of nalidixic acid in waters and wastewaters of different

630 composition. Analytical assessment by LC-TOF-MS. Water Res. 45, 1736–1744.

631 Tahrani, L., Soufi, L., Mehri, I., Najjari, A., Hassan, A., Loco, J.V., Reyns, T., Cherif,

632 A., Mansour, H.B., 2015. Isolation and characterization of antibiotic-resistant bacteria

633 from pharmaceutical industrial wastewaters. Microb. Pathogenesis 89, 54-61.

634 Vasiliadou, I.A., Molina, R., Martinez, F., Melero, J.A., Stathopoulou, P.M., Tsiamis,

635 G., 2018. Toxicity assessment of pharmaceutical compounds on mixed culture from

636 activated sludge using respirometric technique: The role of microbial community

637 structure. Sci. Total Environ. 630, 809–819.

638 Vining, G.G., 2003. Statistical Methods for Engineers, Duxbury Press, Pacific Grove,

639 CA.

640 Yang, S.F., Lin, C.F., Lin, A.Y.C., Hong, P.K.A., 2011. Sorption and biodegradation of

641 sulfonamide antibiotics by activated sludge: Experimental assessment using batch data

642 obtained under aerobic conditions. Water Res. 45, 3389-3397.

643 Zhang, X., Zhang, T., Fang, H.P., 2009. Antibiotic resistance genes in water

644 environment. Appl. Micobiol. Biotechnol. 82, 397-414.

645 Zhang, S., Han, B., Gu, J., Wang, C., Wang, P., Ma, Y., Cao, J., He, Z., 2015. Fate of

646 antibiotic resistant cultivable heterotrophic bacteria and antibiotic resistance genes in

647 wastewater treatment processes. Chemosphere 135, 138–145.

648

649

650

651

652 **Figure captions**

653 Figure 1. Flowchart of the WWTP of Villapérez (Asturias, Spain) for municipal

654 wastewater treatment.

655 Figure 2. Degradation rate for carbon source ($r_{su,H}$) (a), net heterotrophic biomass

656 growth rate ($r'_{x,H}$) (b), degradation rate for ammonium source ($r_{su,A}$) (c), and net

657 autotrophic biomass growth rate ($r'_{x,A}$) (d) in absence and presence of nalidixic acid

658 (NAL) for the three operation periods. Data are mean of three replicates and error bars

659 represent standard deviation.

660 Figure 3. Triplot diagram for redundancy analysis (RDA) of the kinetic parameters (Y,

661 μ_m, K_S and b), substrate degradation rate (r_{su}) and net biomass growth rate (r'_x) in

662 relation to the operation variables HRT, X_{VSS}, T and SRT for heterotrophic biomass in

663 absence of nalidixic acid (NAL) (a) and presence of NAL (b), and for autotrophic

664   biomass in absence of NAL (c) and presence of NAL (d) within the NIPHO activated

665   sludge reactor.

666

667

668
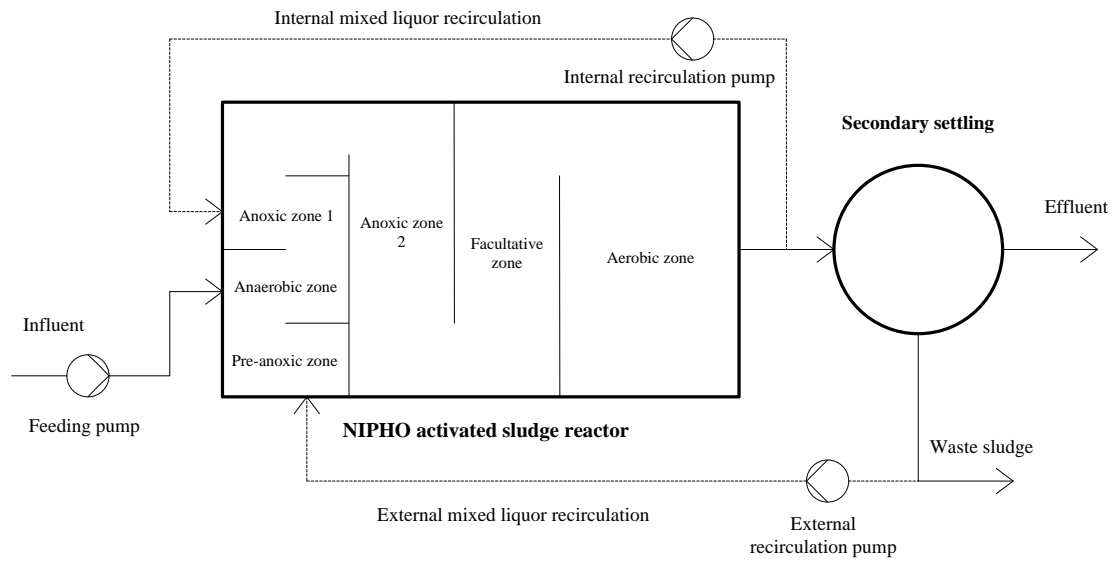
669
670
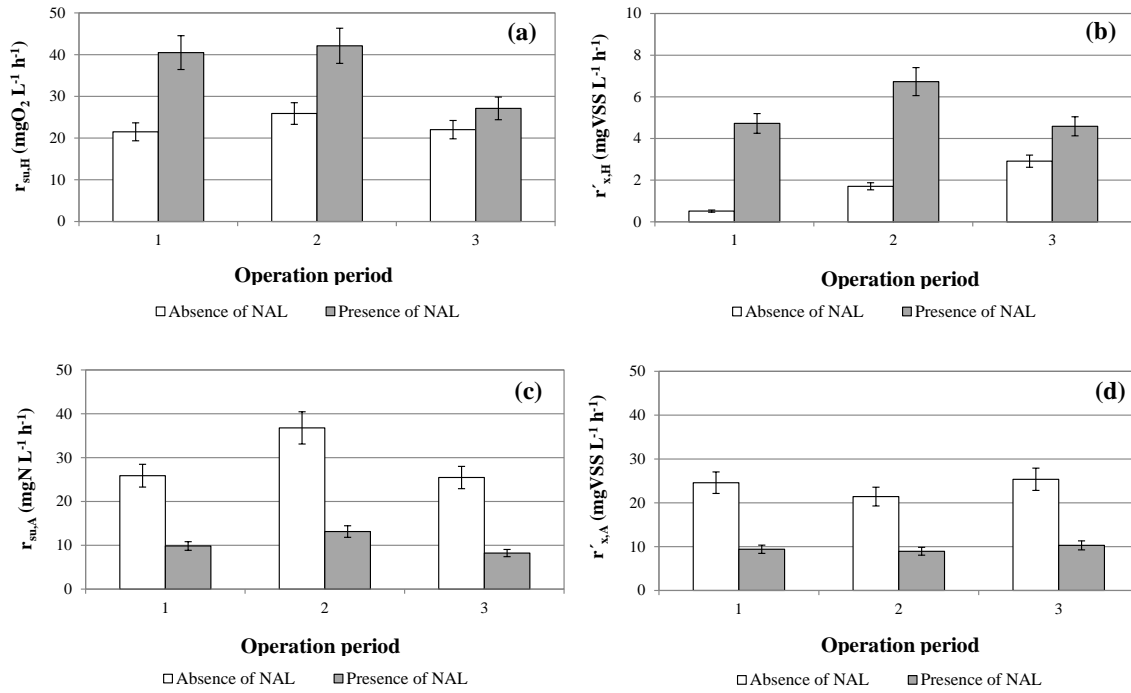671   **Figure 1**

672
673

674

675
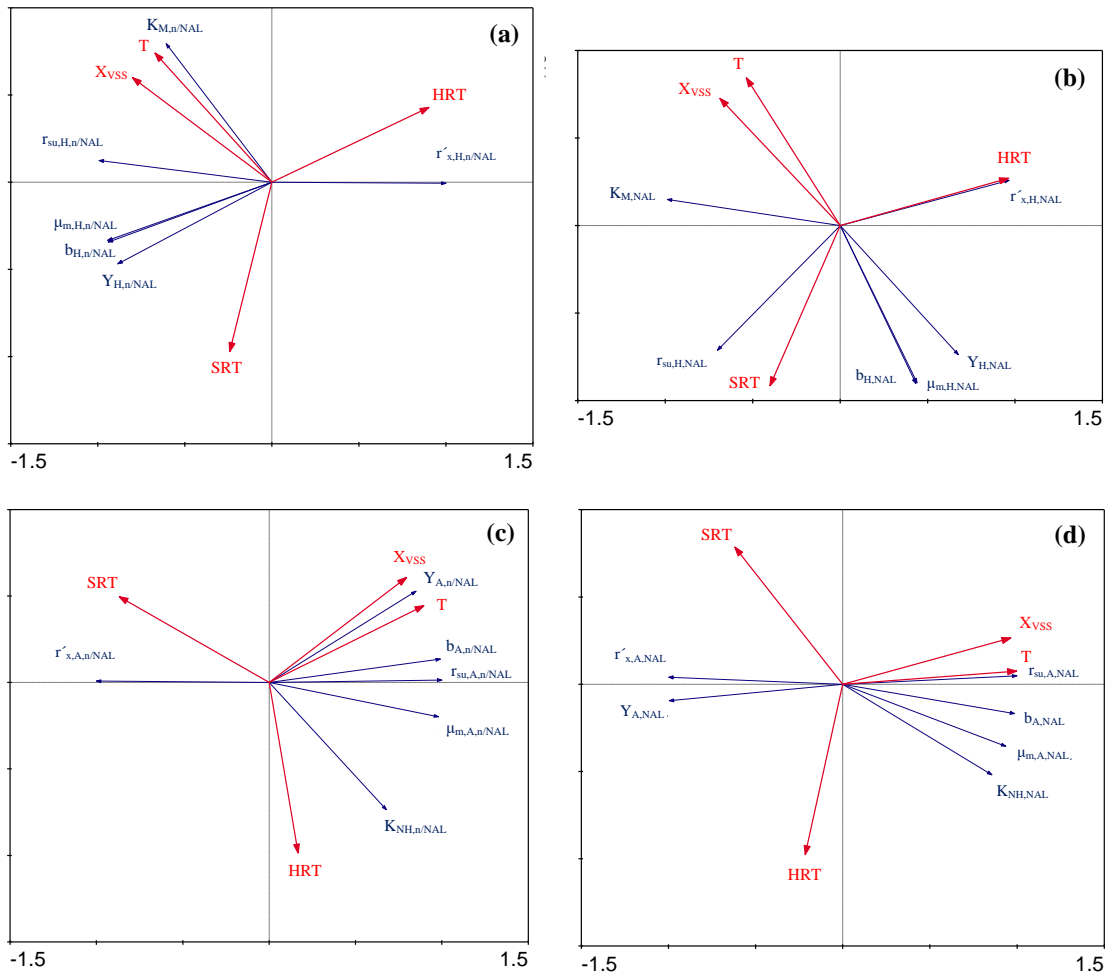
676

677

678

679

680

681

Figure 2

Figure 3

686

687

688

689

690

691

692

693

694

695

696

697

698

699

700

Tables

Table 1. Kinetic parameters for heterotrophic and autotrophic biomass in absence and presence of nalidixic acid (NAL) for the three operation periods of the NIPHO activated sludge reactor.

Parameter	Operation period		
	1	2	3
HETEROTROPHIC KINETICS			
Absence of NAL			
$Y_{H,n/NAL}$ (mgVSS mgCOD^{-1})	0.4252±0.0358	0.3596±0.0388	0.4071±0.0432
$\mu_{m,H,n/NAL}$ (h^{-1})	0.0060±0.0007	0.0061±0.0009	0.0068±0.0008
$K_{M,n/NAL}$ (mg O$_2$ L^{-1})	0.1390±0.0249	1.1513±0.1342	0.3465±0.0548
$b_{H,n/NAL}$ (day^{-1})	0.1342±0.0129	0.1106±0.0098	0.0913±0.0099
Presence of NAL			
$Y_{H,NAL}$ (mgVSS mgCOD^{-1})	0.2828±0.0111	0.3154±0.0323	0.3686±0.0411
$\mu_{m,H,NAL}$ (h^{-1})	0.0086±0.0009	0.0093±0.0011	0.0080±0.0009
$K_{M,NAL}$ (mgO$_2$ L^{-1})	6.3391±0.6479	5.3233±0.3286	1.9073±0.1986
$b_{H,NAL}$ (day^{-1})	0.0854±0.0058	0.0771±0.0109	0.0696±0.0065
AUTOTROPHIC KINETICS			
Absence of NAL			
$Y_{A,n/NAL}$ (mgVSS mgN^{-1})	1.2281±0.1508	0.7255±0.0520	1.3434±0.1226
$\mu_{m,A,n/NAL}$ (h^{-1})	0.2749±0.0323	0.2239±0.0187	0.6614±0.0630
$K_{NH,n/NAL}$ (mgN L^{-1})	0.8779±0.0815	0.7298±0.0892	1.5615±0.1486
$b_{A,n/NAL}$ (day^{-1})	0.0587±0.0069	0.0816±0.0086	0.1133±0.0091
Presence of NAL			
$Y_{A,NAL}$ (mgVSS mgN^{-1})	1.2428±0.1290	0.8573±0.0796	1.7017±0.1611
$\mu_{m,A,NAL}$ (h^{-1})	0.1010±0.0097	0.0912±0.0081	0.2334±0.0176
$K_{NH,NAL}$ (mgN L^{-1})	0.2128±0.0161	0.2195±0.0312	0.3900±0.0286
$b_{A,NAL}$ (day^{-1})	0.0360±0.0048	0.0569±0.0059	0.0898±0.0074

Table 2. Mathematical modeling and optimization of heterotrophic and autotrophic kinetics for the NIPHO activated sludge reactor in absence and presence of nalidixic acid (NAL).

Fitting parameter	Heterotrophic kinetics (H)		Autotrophic kinetics (A)	
	Absence of NAL	Presence of NAL	Absence of NAL	Presence of NAL
$\lambda_{1,H/A}$	-0.00377	0.05895	-0.14472	-0.01785
$\lambda_{2,H/A}$	0.00002	0.00001	-0.00506	-0.00715
$\lambda_{3,H/A}$	0.00181	0.00519	-0.00718	0.00517
$\lambda_{4,H/A}$	0.00001	-0.00001	0.00001	0.00001
$\lambda_{5,H/A}$	0.02416	0.00370	0.15822	0.15029
R^2	0.97085	0.97482	0.99913	0.99973
$\gamma_{1,H/A}$	-0.00424	0.01690	-1.92146	-0.85544
$\gamma_{2,H/A}$	0.00023	-0.00199	6.42573	3.87542
$\gamma_{3,H/A}$	0.00668	-0.01356	0.78239	0.65367
$\gamma_{4,H/A}$	-0.00012	0.00133	-9.01171	-1.85340
$\gamma_{5,H/A}$	-0.00570	0.17993	-8.33858	-4.98311
R^2	0.99700	0.99780	0.99997	0.99990
$\varphi_{1,H/A}$	0.31647	-2.02909	0.11956	0.05468
$\varphi_{2,H/A}$	0.00208	0.00900	-0.00724	-0.00135
$\varphi_{3,H/A}$	0.01107	-0.14500	0.01657	0.00616
$\varphi_{4,H/A}$	0.00002	-0.00019	-0.00001	-0.00001
$\varphi_{5,H/A}$	-0.31326	-0.22895	0.09714	0.01374
R^2	0.98063	0.99871	0.99970	0.99942
$\alpha_{1,H/A}$	0.46998	0.20145	-0.39817	-0.39754
$\alpha_{2,H/A}$	-0.01946	-0.01063	0.56121	0.71279
$\alpha_{3,H/A}$	-0.19326	-0.07797	0.23255	0.22925
$\alpha_{4,H/A}$	-0.02414	0.02511	-0.14763	-0.15376
$\alpha_{5,H/A}$	1.64494	0.91491	-0.64990	-0.85104
R^2	0.99975	0.99973	0.99982	0.99927
Optimum operational conditions				
HRT (h)	3.8	2.8	3.8	3.8
X_{VSS} (mgVSS L^{-1})	1,566	1,566	125	125
T (ºC)	12.6	14.8	12.6	12.6
SRT (day)	12.6	11.0	12.6	12.6
Optimum response				
Y_H (mgVSS mgCOD^{-1})	0.3291	0.2150	-	-
$\mu_{m,H}$ (h^{-1})	0.0051	0.0088	-	-
K_M (mgO$_2$ L^{-1})	0.5272	5.7529	-	-
b_H (day^{-1})	0.0606	0.0773	-	-
$r_{su,H}$ (mgO$_2$ L^{-1} h^{-1})	23.96	54.52	-	-
$r´_{x,H}$ (mgVSS L^{-1} h^{-1})	3.93	6.68	-	-
Y_A (mgVSS mgN^{-1})	-	-	0.8013	0.9342
$\mu_{m,A}$ (h^{-1})	-	-	0.4835	0.1676
K_{NH} (mgN L^{-1})	-	-	0.7863	0.2174
b_A (day^{-1})	-	-	0.0834	0.0656
$r_{su,A}$ (mgN L^{-1} h^{-1})	-	-	69.21	22.02
$r´_{x,A}$ (mgVSS L^{-1} h^{-1})	-	-	55.02	20.23